TECHNICAL NOTE

# Clearing strategies for 3D spheroids.

**We demonstrate:**

- How to increase imaging depth in 3D spheroids by a factor of four
- How different optical clearing techniques affect clearing effectiveness, clearing time and spheroid morphology

## Authors

Stefan Letzsch
Karin Boettcher
Alexander Schreiner

Revvity, Inc.



## Abstract

Multicellular spheroids have emerged as powerful tools to bridge the gap between *in vitro* cell culture models and *in vivo* tissues. In drug discovery programs, where high-throughput is required, investigators to date have been unable to take full advantage of these models because of the lack of available methods to fully interrogate them. Perhaps the greatest challenge in higher throughput 3D imaging is the acquisition of images of solid spheroids, owing to the reduced light penetration from increased light absorption and scattering properties. One solution is to use optical clearing techniques, which can enhance the imaging depth in spheroids by removing lipid and protein molecules, which contribute to light scattering effects, and by modifying the refractive indices within the sample.

In this technical note, we compare different optical clearing strategies for 3D spheroids using the Opera Phenix® Plus high-content screening system and quantify the clearing effectiveness and alterations in spheroid morphology using Harmony® imaging and analysis software.

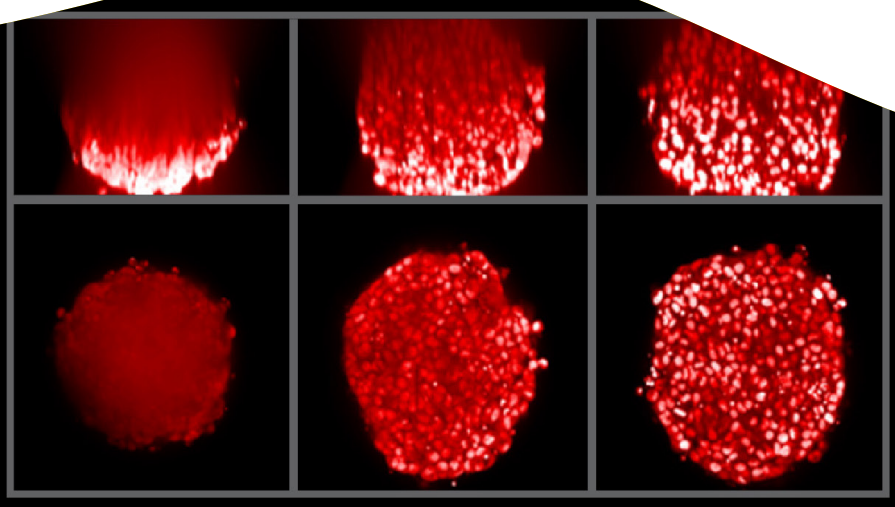

## Spheroid production and optical clearing

To create spheroids, approximately 500 HeLa cells per well were seeded in CellCarrier™ Spheroid Ultra Low Attachment (ULA) 96-well microplates (Revvity, #6055330). After 3 days in culture at 37 °C and 5% $CO_2$, spheroids were fixed with 3.7% formaldehyde. The diameter of the spheroids was approximately 250 µm. Nuclei were stained with 5 µM DRAQ5™ for 1 h at room temperature. For imaging, spheroids were manually transferred into a PhenoPlate™ 384-well microplate (Revvity, #6057300) in PBS.

The optical clearing approaches described here have been published previously and are grouped into two categories, aqueous-based and organic solvent-based. The aqueous clearing reagents were ScaleA2, ScaleS4 and ScaleS0 – ScaleS4 (sequential clearing).[1,2] For ScaleA2 and ScaleS4 clearing, the spheroids were directly transferred into the final optical clearing solutions. For the sequential optical clearing approach with ScaleS0 – ScaleS4, spheroids were incubated sequentially in ScaleS0, ScaleS1, ScaleS2, and ScaleS3 for 1 h each. Before the final mounting in ScaleS4, the samples were washed with PBS. All Scale incubations were done at 37 °C to enhance the clearing process.

A mixture of benzyl alcohol and benzyl benzoate (BABB) was used as an example of an organic solvent-based clearing solution.[3] For clearing with BABB, the spheroids were initially dehydrated with a series of 5 minute room temperature incubations in methanol solutions of increasing concentration (25%, 50%, 75%, and 100%). Before the final mounting in BABB, the spheroids were incubated for 5 minutes in a 1:1 BABB/methanol mixture. The full compositions of the optical clearing solutions are summarized in Table 1.

HeLa spheroids were imaged on an Opera Phenix Plus high-content screening system using a 20x water immersion objective (NA 1.0), in the absence or presence of the different clearing reagents. To monitor clearing success over time, confocal image stacks (300 planes, 1 µm z-plane intervals) were acquired after four different time points (1 h, 18 h, 48 h and 96 h). Detection of each individual spheroid was centered in one field of view using the PreciScan intelligent image acquisition tool (available in versions 4.5 or later of Harmony imaging and analysis software).

## Imaging results

As commonly reported, optical clearing techniques significantly increase the imaging depth over time. Without clearing, in PBS, only the lower quarter of a 250 µm thick HeLa spheroid is visible. In contrast, when a clearing method is applied, imaging into the core or even through the entire sphere is achieved (Figure 1). The effectiveness of each of the clearing methods shown in Table 1 is dependent on the cell type, the overall thickness in the z dimension, the ECM substrate used, and the length of time that the clearing agent was applied.

## 3D analysis of spheroids

To quantify the effectiveness of the clearing methods and the morphology of spheroids in the different clearing solutions, the 3D high-content analysis and visualization tools built into Harmony high-content analysis software were used. As a first step in the image analysis process, the visible region of each spheroid was detected using a local intensity threshold. Subsequently, the spheroid region was segmented into individual nuclei. In the uncleared 3D samples, nuclei could only be detected in the outer spheroid region. After successful optical clearing, e.g. using ScaleS4, nuclei were detectable throughout the whole spheroid (Figure 2).

Table 1: Compositions of optical clearing solutions.

| Ingredients | ScaleA2 | ScaleS0 | ScaleS1 | ScaleS2 | ScaleS3 | ScaleS4 | BABB |
|---|---|---|---|---|---|---|---|
| D-(-)-sorbitol (% w/v) | - | 20 | 20 | 27 | 36.4 | 40 | - |
| Glycerol (% w/v) | 10 | 5 | 10 | - | - | 10 | - |
| Urea (M) | 4 | - | 4 | 2.7 | 2.7 | 4 | - |
| Triton X-100 (% w/v) | 0.1 | - | 0.2 | 0.1 | - | 0.2 | - |
| Methyl-β-cyclodextrin (mM) | - | 1 | - | - | - | - | - |
| γ-cyclodextrin (mM) | - | 1 | - | - | - | - | - |
| N-acetyl-L-hydroxyproline (% w/v) | - | 1 | - | - | - | - | - |
| Dimethylsulfoxide (% v/v) | - | 3 | - | 8.3 | 9.1 | 15-25 | - |
| PBS (-) | - | 1x | - | - | 1x | - | - |
| Benzyl alcohol/benzyl benzoate solution | - | - | - | - | - | - | 1:2 ratio |

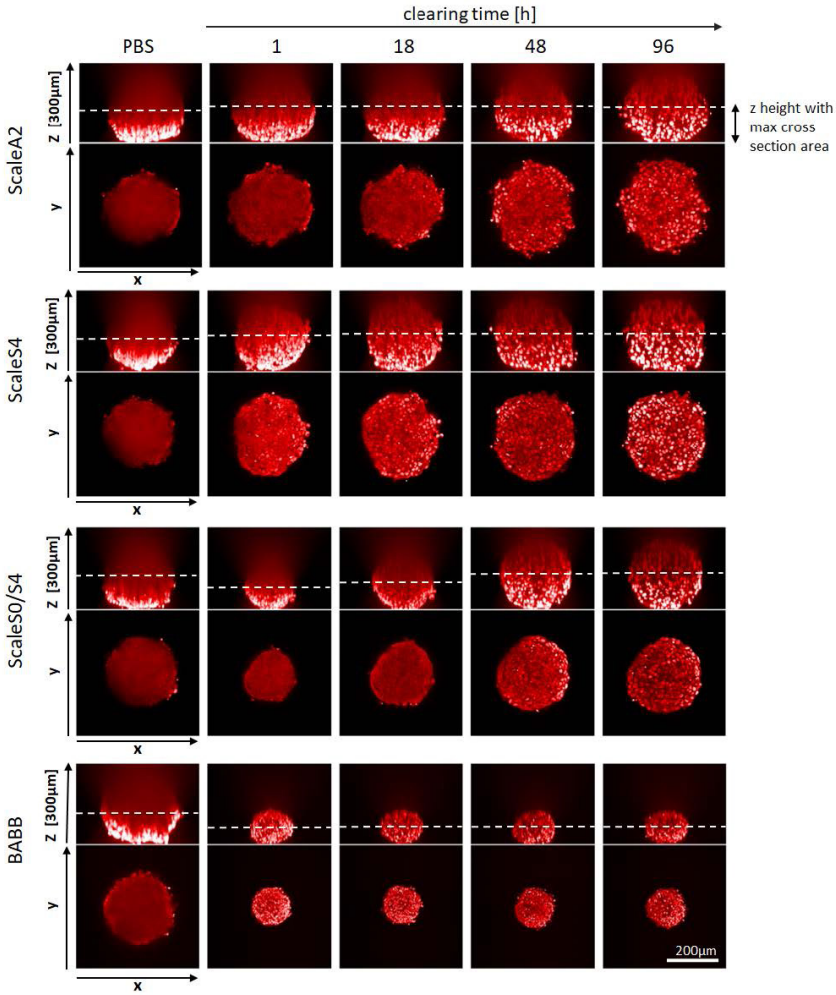


Figure 1: Optical clearing solutions increase imaging depth of spheroids over time. While only the lower quarter of a 250 µm thick spheroid is visible in PBS, imaging beyond this, towards the core or almost completely through the spheroid, was only achieved when a clearing technique was applied. Images show one representative HeLa spheroid per clearing method. The same spheroid was imaged before (in PBS) and at four different time points after the addition of the optical clearing solutions. The x/z dimension images in the upper rows represent longitudinal cuts of spheroids. The x/y dimension images in the lower rows are from the respective z height dimensions with the maximum cross section area, as indicated by the dashed line in the x/z images.

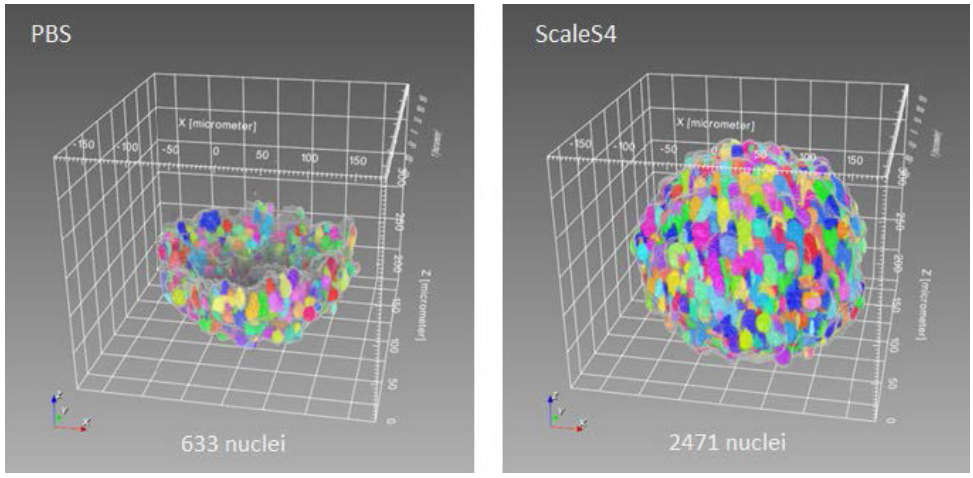


Figure 2: Optical clearing allows the detection of up to four times more nuclei using Harmony software. Image stacks (300 @ 1 µm intervals) were acquired in confocal mode on the Opera Phenix Plus system using a 20x water immersion objective.

In addition to the nuclei count, the mean nuclei volume and the mean DRAQ5™ intensity in the nucleus were calculated. As a readout for the overall optical clearing effectiveness, the "visible fraction" of the spheroids was calculated by dividing the visible height by the spheroid diameter, which can be derived from the maximum cross section area.

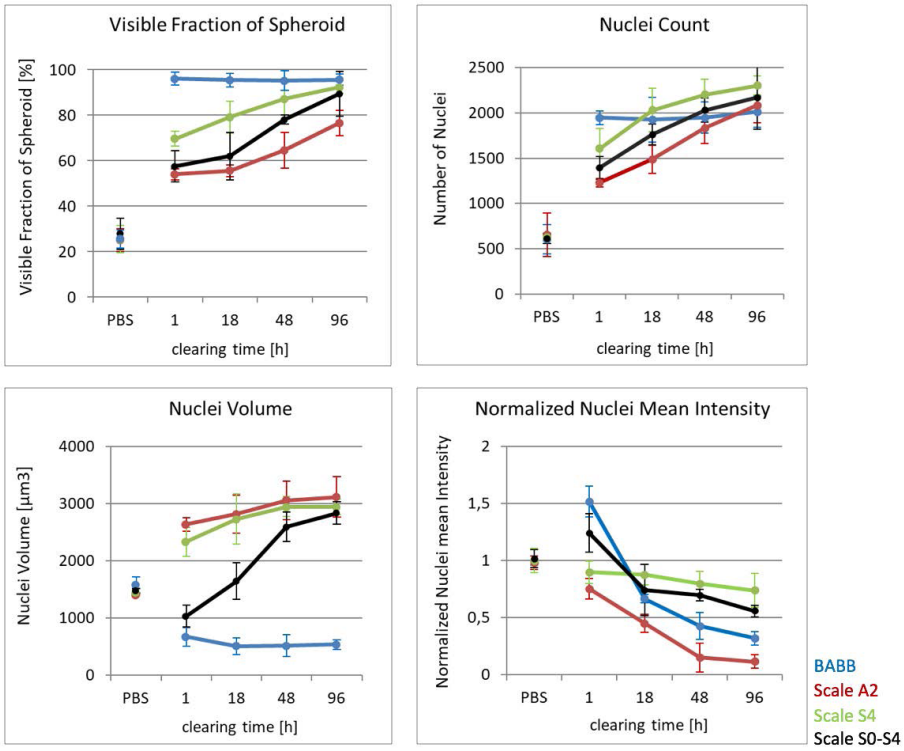


Figure 3: Optical clearing allows image detection deeper into HeLa spheroids but alters nuclear volume and intensity. The visible fraction and nuclei count increase over time for all clearing approaches. The nuclei volume increases for the aqueous-based clearing solutions (Scale) and decreases for the organic solvent-based solution (BABB). The mean intensity of DRAQ5™ in the nucleus decreases for all optical clearing approaches over time; ScaleA2 showed the most significant decrease in mean nuclei intensity compared to other clearing approaches tested in this study. All readouts were calculated with the 3D high-content analysis tools of Harmony software. Data represent at least three individual spheroids and error bars represent the SD.

While the visible fraction of an uncleared spheroid is about 25% in PBS, clearing increases the imaging depth and the ability to segment nuclei with increasing clearing time (Figure 3). For ScaleA2, detection increases to 55% after 1 h and up to 78% after 96 h. For ScaleS4, the clearing process is faster and even more effective, with visibility values of 95% after 96 h. BABB, like other solvent-based clearing solutions, reduces the incubation time necessary to clear spheroids with complete optical clearing in little as 1 h (Figure 3).

While clearing enables imaging of an entire 250 µM Hela spheroid, it is known that clearing agents, such as those described here, modify the spheroid size and intensity properties of nuclei.

The nuclei volume increases after ScaleA2 or ScaleS4 treatment, approximately doubling after 96 h. In contrast to the uncleared spheroid in PBS solution, ScaleS0 initially leads to nuclei shrinkage in spheroids after 1 h, but by transfering spheroids through ScaleS1, ScaleS2, ScaleS3 into ScaleS4, the nuclei volume reaches a comparable size to the other Scale solutions. Due to spheroid dehydration, BABB treatment, similar to other solvent-based clearing agents, leads to shrinkage of the nuclei volume by approximately 66% (Figure 3). This change in nuclei volume corresponds to the change in volume of the whole spheroids (data not shown).

Optical clearing also decreases detection of DRAQ5™ in HeLa spheroids. The largest decrease in fluorescence intensity, observed with ScaleA2 clearing solution, was nearly 80% after 96 h, whereas the fluorescence intensity was reduced by only 40-50% in ScaleS4 or BABB clearing (Figure 3).

## Conclusion

Multicellular spheroids are often characterized by proliferation gradients and cell heterogeneity. Incomplete imaging of the spheroid is therefore a major concern for researchers as it can reduce the possibility of discovering further insights from biologically interesting zones such as the spheroid core (or necrotic core in tumoroids).

Here we have shown that optical clearing, combined with imaging on the Opera Phenix Plus system, improves the imaging depth and the nuclei segmentation in HeLa spheroids by a factor of 4. This improved methodology allows complete imaging of spheroids with a diameter of approx. 250 µm when using water immersion objectives. Several previously published, nonproprietary clearing solutions (aqueous-based and organic solvent-based) were tested. The ScaleS4 method demonstrated the best clearing characteristics with a simple, straightforward protocol. Notably, ScaleS4 leads to an expanded spheroid volume, which is favorable for image analysis segmentation, while retaining fluorescence intensity. However, it shows considerable curing over time, with best results achieved after 48-96 h of incubation. An aqueous-based clearing solution such as ScaleS4 with water immersion objectives is an ideal combination that properly matches the refractive indices to improve 3D image quality and reduce optical aberrations.[5]

Revvity's Opera Phenix Plus and Operetta CLS™ high-content screening systems, together with Harmony imaging and analysis software, are highly-suited to analyze complex 3D cell model systems with integrated image acquisition and 3D software tools to visualize, analyze, and gain insights into the biological content of physiologically more relevant

cell models.

## References


1. Hama, H., Kurokawa, H., Kawano, H., Ando, R., Shimogori, T., and Noda, H. et al. (2011). Scale: a chemical approach for fluorescence imaging and reconstruction of transparent mouse brain. *Nature Neuroscience,* 14(11), 1481-1488. doi: 10.1038/nn.2928

2. Hama, H., Hioki, H., Namiki, K., Hoshida, T., Kurokawa, H., and Ishidate, F. et al. (2015). ScaleS: an optical clearing palette for biological imaging. *Nature Neuroscience,* 18(10), 1518-1529. doi: 10.1038/nn.4107

3. Dodt, H., Leischner, U., Schierloh, A., Jährling, N., Mauch, C., and Deininger, K. et al. (2007). Ultramicroscopy: threedimensional visualization of neuronal networks in the whole mouse brain. *Nature Methods,* 4(4), 331-336. doi: 10.1038/ nmeth1036

4. Boutin, M., Voss, T., Titus, S., Cruz-Gutierrez, K., Michael, S., and Ferrer, M. (2018). A high-throughput imaging and nuclear segmentation analysis protocol for cleared 3D culture models. Scientific Reports, 8(1). doi: 10.1038/ s41598-018-29169-0

5. Boettcher, K., & Schreiner, A. (2017). The Benefits of Automated Water Immersion Lenses for High-Content Screening [Technical Note]. Revvity, Inc.


**Revvity, Inc.**
940 Winter Street
Waltham, MA 02451 USA

(800) 762-4000
www.revvity.com